Pergamon

Acta mater. Vol. 46, No. 11, pp. 3725–3732, 1998

Printed in Great Britain
PII: S1359-6454(98)00098-6
1359-6454/98 $19.00 + 0.00

STABLE STATE OF INTERCONNECT UNDER TEMPERATURE CHANGE AND ELECTRIC CURRENT

Z. SUO

Mechanical and Aerospace Engineering Department and Princeton Materials Institute, Princeton University, Princeton, NJ 08544, U.S.A.

(Received 9 May 1997; accepted 9 March 1998)

Abstract—This paper considers aluminum interconnects in the presence of insulators, vias, and shunts. Subject to a temperature change and a direct electric current, such an interconnect evolves—after a complicated sequence of events—into a stable state with a segment of aluminum depleted near the cathode, a linear distribution of pressure in the rest of the line, and no further mass diffusion. The electric current continues in the shunt layers where aluminum is depleted; the multilayer interconnect never opens, but its resistance has increased to a saturation level. Several aspects of this stable state are discussed, including the condition under which the high pressure near the anode does not cause the surrounding insulator to crack; the dependence of saturation resistance on shapes, materials, and loads; and the time scale for the interconnect to evolve to the stable state. Should a circuit tolerate a variable resistance up to saturation, the interconnect would function forever. Implications of this possibility are also discussed. © *1998 Acta Metallurgica Inc.*

1. INTRODUCTION

On a silicon chip interconnects are made of several levels of aluminum lines. Silicon dioxide fills the space in between to provide insulation. The whole structure is a metal network embedded in an oxide matrix. In addition to aluminum, refractory metals such as tungsten and titanium are pervasive in interconnect structures (Fig. 1). The tungsten studs serve as vias to link aluminum lines between different levels. The titanium aluminide layers shunt the electric current where voids deplete aluminum. The refractory metals allow negligible mass transport, but have high electrical resistivities. A representative aluminum line has a rectangular cross-section of submicron dimensions, and is subject to thermal expansion misfit, electric current, and elevated temperature. The substantial forces acting in a small dimension have caused concerns ever since integrated circuits came into being. Issues evolve as the structures of interconnects miniaturize and become more complex [1–3].

The impact of the insulators, vias, and shunts on interconnect reliability has been a focus of recent studies. Figure 2 summarises the main observations. Upon cooling from the processing temperature (about 400°C), thermal expansion misfit causes a tensile stress in aluminum. Interacting with defects, the stress induces voids [4, 5]. Each void grows and relaxes the stress in its vicinity. Far below the processing temperature, thermal misfit is large but diffusivity is low, so that the aluminum line often has many small voids and some unrelaxed stress.

Once a direct electric current is supplied, electrons enter the aluminum line from one tungsten stud (cathode), and leave from another (anode). The electron wind causes aluminum atoms to diffuse in the direction toward the anode. Atoms may diffuse along many paths: grain boundaries, various interfaces, void surfaces, and the crystal lattice. Under the combined thermal misfit and electron wind, the voids exhibit extraordinarily complex dynamics: they nucleate, disappear, drift, change shape, coalesce, and break up [6, 7].

Despite the commotion in the transient, the end state is simple [8–10]. After a sufficiently long time, only a single void remains near the cathode. Voids in the middle of the line have now been filled or swept into the cathode void. The tungsten studs and the oxide conserve the total number of aluminum atoms in the line. As the void grows, atoms diffuse into the rest of the line, inducing a distribution of pressure. It is the gradient of the pressure that stops electromigration. The interconnect stays in this state afterwards, until the temperature or current changes again.

The main functional characteristic of an interconnect is its resistance. Imagine several identical lines, each carrying a different current. Figure 3 illustrates the resistance change as a function of time. The resistance increases as the void enlarges. Two long-term trends are expected: the resistance either saturates or runs away. Evidently, the larger the current, the higher the saturation resistance. For a line carrying a large current, a large pressure gradient is needed to stop mass diffusion. The high pressure in

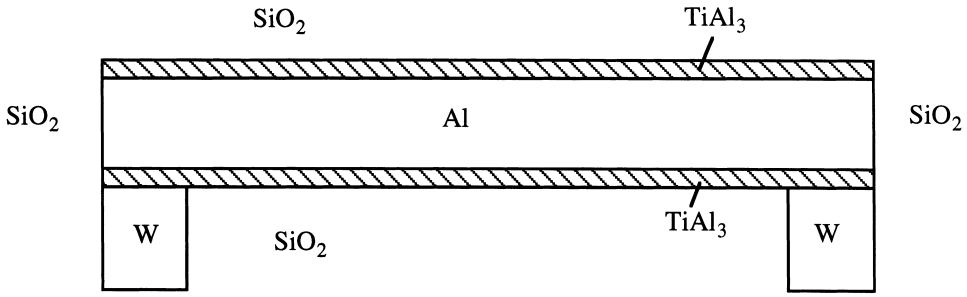

Fig. 1. A schematic of an interconnect, embedded in a silicon dioxide matrix, on a silicon substrate.

aluminum near the anode, in its turn, may cause the surrounding oxide to crack. Once the oxide cracks, aluminum extrudes, diffusion restarts, and the cathode void grows further, so that the resistance increases indefinitely. Cracking may also break down insulation between neighboring lines, leading to a short circuit. Figure 4 sketches two examples of cracks in oxide caused by the pressure in aluminum. The interfaces between various materials in the structure can also debond and allow aluminum to extrude.

The paper discusses three aspects of the stable state. First, the two behaviors of resistance, saturation or run-away, are differentiated by whether the oxide can sustain the electromigration-induced pressure in aluminum. A no-cracking condition is suggested on the basis of fracture mechanics. Second, a circuit can only tolerate a limited resistance change. The dependence of saturation resistance on current density, temperature drop, and line geometry is examined. Third, the interconnect evolves by mass diffusion. The time scale for the interconnect to adapt to newly established temperature and current is discussed. Also discussed is the possibility of using the stable state in circuit design.

2. NO-CRACKING CONDITION

2.1. Assumption of hydrostatic state

The stress field in an aluminum line is complicated in general. Upon cooling from the processing temperature, thermal expansion misfit induces triaxial tensile stresses in the aluminum line. Many models assume that aluminum in such a small dimension still behaves like a von Mises solid, with a temperature-dependent yield strength [11–13]. They predict non-hydrostatic stresses in the aluminum line. On the other hand, diffusion relocates mass among various grain boundaries and interfaces (e.g. the Herring or Coble creep), and over some time relaxes the line to a hydrostatic state. This hydrostatic state is independent of the details of plasticity or diffusion, and can be calculated from an elasticity problem. The predictions of various models have been compared in [14].

After a void appears, or an electric current is supplied, the stress becomes nonuniform along the line. Kohennen *et al.* [15] argued that, on the time scale of an electromigration test, the Herring or Coble creep rapidly relaxes each point in the line to a hydrostatic state. Consequently, to study mass

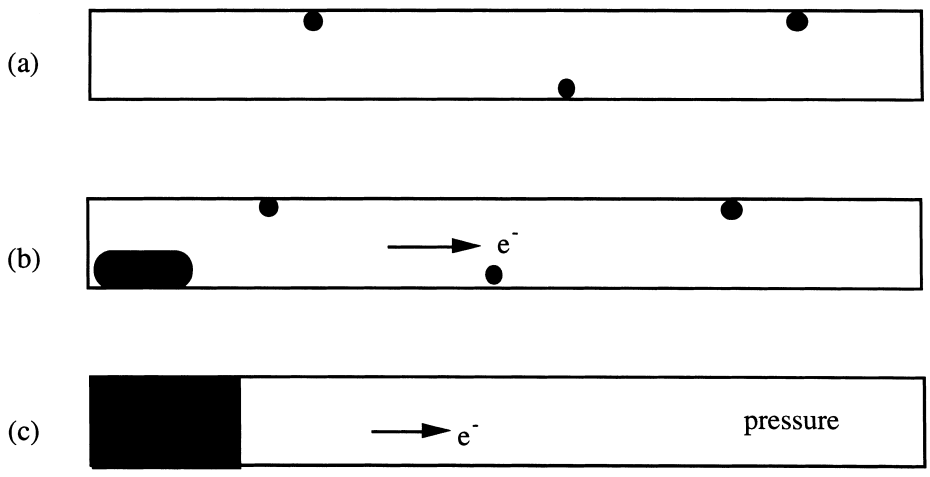

Fig. 2. (a) Upon cooling from the processing temperature, voids form to partially relax thermal stress. (b) Subject to a current, atoms diffuse toward the anode, and a void grows at the cathode end. (c) The line reaches the stable state, with a single void left at the cathode end, a linear pressure distribution in the rest of the line, and no further mass diffusion.

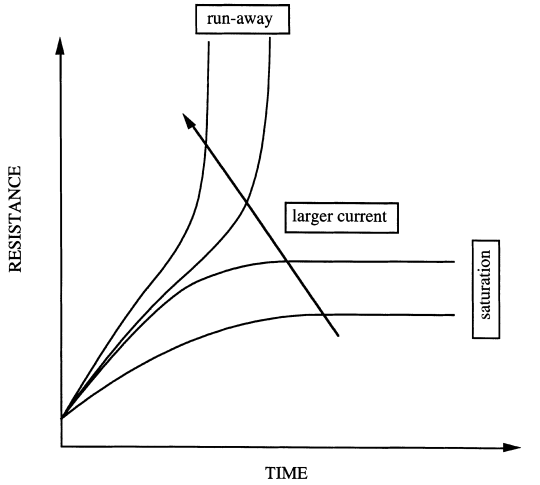

Fig. 3. Resistance increases as a function of time. Under a small current, the resistance saturates. Under a large current, the resistance runs away.

transport events in the line over a length exceeding several times the linewidth, one can assume that the stress state is hydrostatic, varying along the line and with time. A recent simulation has confirmed that this assumption gives good predictions, provided the grain size is much smaller than the line length [16].

This paper adopts the assumption of hydrostatic state. It is represented by a pressure; a tensile stress corresponds to a negative pressure. Let the x axis coincide with the line, from the cathode to the anode, $0 < x < L$, L being the length of the aluminum line. The pressure is a function of position and time, $p(x, t)$. Figure 5 sketches pressure distributions in several circumstances. Upon cooling, thermal misfit induces a uniform tensile stress along the line. Once a void appears, the tensile stress is relaxed in its vicinity. As the void enlarges, the stress is relaxed in a growing segment of the line. When an electric current is supplied, after a complicated sequence of events, the line evolves to a stable state, with a single void near the cathode, and a linear pressure distribution of the rest of the line. Because this state is central to the present paper, the following subsection reviews its details.

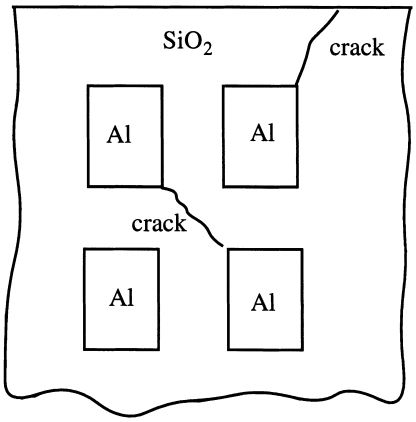

Fig. 4. Cracks in oxide induced by the pressure in aluminum.

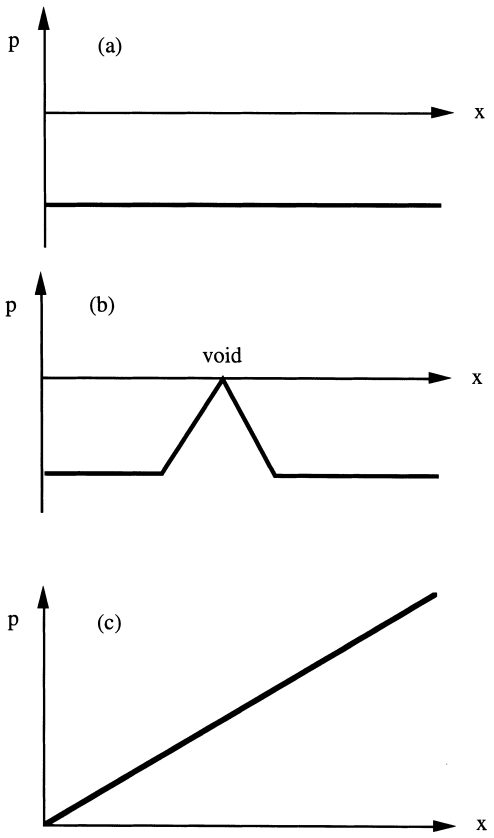

Fig. 5. Pressure distributions in an aluminum line under several circumstances. (a) The stress is tensile and uniformly distributed in a line cooled from the processing temperature. (b) A void releases the tensile stress in its vicinity. (c) A linearly distributed pressure stops electromigration.

2.2. The Blech condition

The electron wind force per atom is proportional to the current density, written as $Z^*e\rho j$, where e is the elementary charge, ρ the resistivity of aluminum, and j the current density. The dimensionless number, Z^*, is determined experimentally; methods on the basis of the stable state will be discussed later. The electron wind force directs to the anode. The driving force per atom due to the pressure gradient is $\Omega\partial p/\partial x$, where Ω is the volume per atom. As stated before, the transient state is complicated; its dynamics need not concern us here. Blech [17] pointed out that mass diffusion stops when the pressure gradient counteracts the electron wind force:

$$\Omega\frac{\partial p}{\partial x} = Z^*e\rho j. \tag{1}$$

Consequently, in equilibrium, the pressure is linearly distributed along the line. The situation is analogous to a liquid subject to gravity, where the pressure increases linearly with the depth.

The void makes the pressure vanish at the cathode, i.e. $p = 0$ at $x = 0$. The capillary pressure is negligible. Aluminum near the anode sustains the highest pressure, denoted by p_A. Integrating (1), one finds the equilibrium pressure distribution,

$$p(x) = p_A \frac{x}{L}, \tag{2}$$

and the anode pressure,

$$p_A = \frac{Z^* e \rho}{\Omega} jL. \tag{3}$$

Observe that the equilibrium pressure is unaffected by the temperature, to the extent that the temperature dependencies of the materials constants in (3) are negligible.

Equation (3) gives the anode pressure needed to stop electromigration. Its magnitude can be huge. In a recent paper [9], it was stated that for 100 μm lines tested under various current densities, aluminum did not extrude under 0.56×10^{10} A/m^2, but did under 1.0×10^{10} A/m^2. Using $L = 100\,\mu$m, $j = 1.0 \times 10^{10}$ A/m^2, $Z^* = 5$, $e = 1.6 \times 10^{-19}$C, $\rho = 3 \times 10^{-8}$ Ωm, and $\Omega = 1.66 \times 10^{-29}$m^3, one finds from (3) that the pressure needed to crack the oxide is $p_A = 1.5$ GPa. The values of j and Z^* used above are not accurately known. These uncertainties aside, it appears inevitable that electromigration will induce tensile stresses in the oxide that are much larger than typical strength of the oxide in bulk. It remains to be ascertained that such high stresses do not break the oxide in the small dimension.

2.3. No-cracking condition for small objects

Fracture mechanics, in its best known form, dictates that the stress needed to cause fracture depends on flaw size. This form is tailored for applications to bulk materials, where the stress is nearly uniform over the scale of flaw size. Two difficulties are evident when applying it to interconnect structures. First, in the presence of inhomogeneity, the stresses at corners are high, possibly singular. Second, the flaw location and size associated with processing are unknown. Fracture mechanics has so far not been used to analyze interconnect structures.

The smallness of the features allows a modified approach, which is less appreciated but equally well grounded within fracture mechanics. It has been developed to analyze cracking induced by thermal expansion misfit in systems containing inclusions, fibers, and thin films [18–21]. In such a system tensile stress is localized, and the associated elastic energy mainly stores in a volume comparable to the size of the small object. When a crack forms, the system releases some elastic energy, but gains surface energy. Thermodynamics dictates that the crack should not form if the elastic energy released is less than the surface energy gained. The elastic energy scales with the volume, and the surface energy scales with the area. When the feature size is small, the volume-to-area ratio is also small, so that the elastic energy stored in the system is insufficient to cause cracking. Under this condition, no flaw can grow, regardless its size, orientation, or location. The no-cracking condition so established is independent of the detailed description of flaws. Nor does the singular stress field at a corner cause any particular concern, because the stress is high only in a small volume, and the total amount of elastic energy is finite.

Analogous to systems containing other small objects [18–21], the oxide around an interconnect cannot crack if

$$\beta p_A \sqrt{w} < K_c, \tag{4}$$

where K_c is the fracture toughness of the oxide, w a characteristic length of the anode geometry, chosen to be the linewidth, and β a dimensionless parameter depending on ratios of various elastic moduli and lengths that describe the anode. The parameter β has been calculated for many small objects [19–21]. Calculations for interconnects will be reported elsewhere. This no-cracking condition is based on the flaw that has the largest elastic energy release rate. Consequently, it is a conservative criterion: if (4) is satisfied, no flaw can grow; if (4) is violated, some flaws grow and others do not. Such a conservative criterion particularly suits integrated circuits, where failure probability of each interconnect must be kept exceedingly low.

As stated above, because the cross-sectional dimension is small, the oxide can sustain a large stress. Taking representative values $\beta = 0.5$, $K_c = 0.5$ MPa $\sqrt{\text{m}}$, and $w = 0.5\,\mu$m, one finds from (4) that the oxide can sustain anode pressure up to $p_A = 1.4$ GPa. That this value is close to the electromigration-induced pressure estimated above is fortuitous. However, both (3) and (4) are robust in that they are insensitive to details. They should give correct orders of magnitude with the reasonable input values.

Combining (3) with (4), one obtains the condition under which the electron wind cannot cause insulator to crack:

$$\beta \sqrt{w} jL < \frac{K_c \Omega}{Z^* e \rho}. \tag{5}$$

The right-hand side collects physical constants, and the left-hand side experimental variables. This condition sets the upper bound on the product jL, once β is calculated and other quantities are measured. For a fixed current density, a shorter line with a small cross-section is safer. Because β depends on the anode geometry and elastic moduli, a systematic

calculation would rank possible shapes and materials. The condition can also be used to estimate Z^* from an experimentally measured current density that causes resistance run-away.

As mentioned before, aluminum may cause debonding along the interfaces between various materials. A condition similar to (5) can be established based on the fracture resistance of the interfaces.

In the above, thermal stresses in the oxide have been ignored. Upon cooling from the processing temperature, a large compressive hoop stress arises in the oxide, resulting from the thermal expansion misfits between the aluminum and the oxide, and between the silicon substrate and the oxide. When an electric current is supplied, the volume of aluminum near the anode increases, which first compensates its thermal contraction, and then goes beyond. Consequently, in the stable state, the stress in the oxide is due to the pressure in the aluminum, and the thermal misfit between the oxide and the silicon substrate. The latter is negligible.

Two other circumstances should be mentioned in this connection. Some dielectrics may develop large intrinsic stresses at the deposition temperature. They are unrelated to the volume change of aluminum, and persist under temperature change and current. A second circumstance involves a line tested under a current up to the stable state, and then brought to a higher temperature. Instantaneously the thermal expansion misfit between aluminum and oxide adds more tensile stress in the insulator. In such cases, the additional stresses must be included in the no-cracking condition.

3. SATURATION RESISTANCE

Saturation resistance has been calculated in [9], [10] and [15]. Here we revisit various assumptions involved in the calculation.

3.1. Saturated void volume

The tungsten studs and the oxide prevent mass from entering or leaving the aluminum line. The total number of aluminum atoms in the line is conserved at all times. The thermal misfit strain is accommodated by a combination of void space and elastic deformation. This allows the void volume to be calculated. First consider a line subject to a temperature drop alone. Imagine separately a free standing aluminum wire, and a tubular cavity in the oxide that should have been occupied by the wire. When the temperature drops from the processing temperature by ΔT, both the wire and the cavity contracts. The volume strain of the aluminum wire is $3\alpha_{\mathrm{Al}}\Delta T$, where α_{Al} is the thermal expansion coefficient of aluminum. The relative volume change of the cavity is $3\alpha_{\mathrm{eff}}\Delta T$, where α_{eff} is an effective thermal expansion coefficient of a value between those of the oxide and the silicon substrate, which can be computed by using the finite element method [14]. The misfit volume strain between the wire and the cavity is $3(\alpha_{\mathrm{Al}}-\alpha_{\mathrm{eff}})\Delta T$. Because aluminum has a much larger thermal expansion coefficient than either the oxide or the silicon substrate, the exact value of α_{eff} is unimportant in estimating the misfit.

Now allow the wire to reside in the cavity. Let the total void volume be V_1 and the aluminum line volume be V. When the stress in the line is completely relaxed, the thermal expansion misfit is fully accommodated by the void space, so that

$$\frac{V_1}{V} = 3(\alpha_{\mathrm{A1}} - \alpha_{\mathrm{eff}})\Delta T. \tag{6}$$

Taking $\alpha_{\mathrm{Al}}-\alpha_{\mathrm{eff}} = 20\times 10^{-6}\ \mathrm{K}^{-1}$ and $\Delta T = 200\ \mathrm{K}$ (corresponding to the drop from the processing temperature to a temperature typical for an electromigration test), one finds from (6) that $V_1/V = 1.2\%$.

Typically, many thermal voids nucleate along the line, each growing to relax stress in its vicinity. Once the stress is completely relaxed throughout the aluminum line, the sum of the volumes of all the voids remains constant afterwards. Equation (6) gives this sum. The actual void volume can be larger or smaller. When a line is cooled to a low temperature for a short time, the tensile stress is not completely relaxed, so that the total void volume will be smaller than that given by (6). After a long time at the low temperature, the stress is completely relaxed, and so the void volume is given by (6). If the line is then brought to a high temperature, for some time the aluminum is under compression, and the void volume is larger than that given by (6).

Next consider a line subject to an electric current alone. In the stable state, atoms that previously occupied the void space have now diffused into the rest of the line, inserted at the grain boundaries or the interfaces, and accommodated by elastic deformation. Consider a slice of material, of thickness $\mathrm{d}x$, cut normal to the line. Let A be the cross-sectional area of the aluminum line, and $\Delta \mathrm{d}x$ be the volume of atoms inserted into the slice. Define an effective elastic modulus B by

$$\frac{\Delta}{A} = \frac{p}{B}. \tag{7}$$

Because a representative aluminum line has a much larger length than the linewidth, B can be calculated from a two-dimensional elasticity problem. In Ref. [15], this modulus is estimated by using elliptic inclusion solutions. For a realistic geometry, it can be calculated by using the finite element method [14].

The void volume equals the total volume of atoms inserted in the line:

$$V_1 = \int_0^L \Delta \mathrm{d}x. \tag{8}$$

In equilibrium, pressure is linearly distributed along the line, equation (2), and so is Δ according to (7). Integrating, one obtains that

$$\frac{V_1}{V} = \frac{p_A}{2B} = \frac{Z^* e\rho}{2\Omega B} jL. \tag{9}$$

The relative void volume, V_1/V, is on the order of elastic strains. Taking $p_A = 1.5$ GPa and $B = 50$ GPa, one finds from (9) that $V_1/V = 1.5\%$.

Finally consider the combined effect of temperature change and electron wind. If the line is held at a temperature below the processing temperature for a long time, even without the electric current, surface energy causes voids to coarsen. The lowest energy state is a single large void. In practice, however, coarsening is a slow process; in the absence of electric current, the aluminum line is typically in a nonequilibrium state with many small voids. Once a direct current is supplied, void coarsening accelerates. The current gradually builds up a pressure field in the line, the small voids are either filled or swept into the large void at the cathode. In the end, only one void remains. Its volume is the sum of those due to thermal misfit and electric current, equations (7) and (9). This void resides at the cathode end, Fig. 2(c). Let L_1 be the length of the void in equilibrium. Evidently, $L_1/L = V_1/V$, so that

$$\frac{L_1}{L} = 3(\alpha_{A1} - \alpha_{eff})\Delta T + \frac{Z^* e\rho}{2\Omega B} jL. \tag{10}$$

The contribution to L_1/L by the temperature drop is independent of the line length, and that by the current is linear in the line length. In the above, we have ignored the volume change due to chemical reaction between aluminum and titanium. It would be interesting to study the beneficial effect of any volume expansion on electromigration lifetime.

The equilibrium void length suggests an experimental method to measure Z^*. Using a known current density, one can ascertain the stable state by resistance saturation. The void length may be measured *in situ* if possible, or by removing the oxide after the electromigration test. Repeat the test using several current densities or line lengths, and plot L_1/L against jL. The slope gives Z^*, assuming that B has been calculated for the line geometry used in the tests.

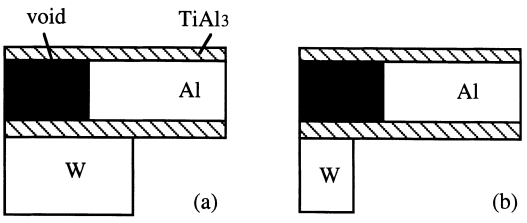

Fig. 6. (a) Void length smaller than tungsten stud diameter. (b) Void length larger than tungsten stud diameter.

3.2. Saturation resistance

The resistance change does not uniquely relate to the void volume. For example, before an electric current is supplied, thermal voids have a significant total volume, but are small and isolated. They do not cause as much resistance increase as a single large void that depletes a segment of the aluminum line. Even when only one void is left at the cathode end, the resistance change depends on geometry. Figure 6 compares two identical voids, the only difference being the size of the tungsten studs relative to the void. Evidently, the resistance increase in Fig. 6(a) is smaller than that in Fig. 6(b).

When the void length exceeds several times the linewidth, the resistance increase can be accurately estimated from the void length [9, 10, 22, 23]. The resistance of a void-free interconnects is $R = \rho L/A$, ignoring the conductance due to the aluminide layers. Let ρ_1 and A_1 be the resistivity and the cross-sectional area of the aluminide layers. When a void of length L_1 appears in the line, current flows in the aluminide layers, and the resistance increases by $\Delta R = \rho_1 L_1/A_1$, where the resistance of aluminum of length L_1 is neglected. Consequently, the relative resistance increase is

$$\frac{\Delta R}{R} = \frac{\rho_1 L_1/A_1}{\rho L/A}. \tag{11}$$

Everything else being equal, the thicker the shunt layers, the smaller the resistance change. Taking $\rho_1/\rho = 10$, $A_1/A = 0.1$, and $L_1/L = 1.0\%$, one finds that $\Delta R/R = 100\%$. Consequently, even under a small current density, the small thermal voids can be swept to the cathode, giving enough void space in the stable state to double the resistance.

Let the saturation resistance change be ΔR_S. A combination of (10) and (11) gives

$$\frac{\Delta R_s}{R} = \frac{\rho_1/A_1}{\rho/A}\left[3(\alpha_{A1} - \alpha_{eff})\Delta T + \frac{Z^* e\rho}{2\Omega B} jL\right]. \tag{12}$$

The experimentally measured saturation resistance can also be used to determine Z^*. Compared to the method based on the void length, this method is simpler in practice, but may have a greater uncertainty if the void length is not much larger than the linewidth.

4. TIME SCALE

To plan experiments, one would like to know the time scale over which an interconnect reaches the stable state. The essential result is contained in Ref. [15], as summarized below for completeness. Let J be the volume flux, i.e. volume of atoms crossing per unit area per unit time. Mass conservation requires that

$$\frac{\partial \Delta}{A\partial t} + \frac{\partial J}{\partial x} = 0. \tag{13}$$

Both the electron wind and the pressure gradient drive the volume flux:

$$J = \frac{D}{kT}\left(Z^* e\rho j - \Omega\frac{\partial p}{\partial x}\right). \tag{14}$$

Here D is the effective diffusivity, k Boltzmann's constant, and T the absolute temperature. Note that the flux vanishes under the Blech condition (1). For simplicity in this discussion, the diffusivity is taken to be uniform along the aluminum line. A combination of (7), (13) and (14) gives

$$\frac{\partial p}{\partial t} = \frac{DB\Omega}{kT}\frac{\partial^2 p}{\partial x^2}. \tag{15}$$

This partial differential equation, together with suitable initial and boundary conditions, governs the evolving pressure distribution, $p(x, t)$. Solutions of practical interest can be found in [15].

Equation (15) is identical to the usual diffusion equation, with the diffusivity-like quantity $DB\Omega/kT$. A dimensional consideration dictates that the time scale for any event involving mass transport over the entire line length, L, be

$$\tau = \eta\frac{L^2 kT}{DB\Omega}, \tag{16}$$

where η is a dimensionless number depending on the chosen event, e.g. attaining a half of the saturation void length. Note that the time scale is independent of the current density. A large current density transports mass at a high rate, but also needs to transport more mass to reach the stable state. The diffusivity is sensitive to temperature and microstructure, and so is the time scale. To accelerate experiments, one may use short lines at high temperatures. The estimate (16) assumes that void nucleation at the cathode end is fast compared to mass transport over the line length.

5. IMMORTAL INTERCONNECT

Provided a circuit tolerates a variable resistance up to its saturation level, an interconnect may function forever. In a private conversation Carl Thompson suggested that such an interconnect be called an immortal interconnect. It becomes immortal by evolving into a stable state to adapt to newly established temperature and current. To what extent a circuit will accept an adaptive interconnect is a complex question, which cannot be answered here. The intent of this brief discussion is to bring out the attractive features of the stable state, and its key limitations.

Assuming that a circuit can tolerate resistance change up to saturation, the stable state gives a simple perspective on interconnect reliability. One can focus on the stable state itself, rather than the rate processes to reach it. It plays down the roles of the time scale, the rate processes, and the microstructure of aluminum. No longer need the microstructure be optimized for slow mass transport or low void nucleation rate. Nor is performance sensitive to temperature. In short, the reliability is warranted by energetics, rather than kinetics, and is therefore much more robust.

The use of the stable state is limited in two ways: the insulator may crack, or the saturation resistance may be prohibitively large. The above estimates indicate that the latter is more critical within the current technology. For a short line, the saturation void length L_1 predicted from (10) is small. The final configuration looks like that in Fig. 6(a), giving rise to a small resistance change. Consequently, the stable state may find ready applications in short lines. For a long line, the saturation void is long compared to the diameter of a tungsten stud, so that the saturation resistance increase is given by (11). As stated before, based on the parameters typical in current technology, the saturation resistance change is very large. In principle, however, the resistance change can be lowered with shunt layers of lower resistivity and larger thickness.

6. CONCLUDING REMARKS

When a temperature and a current is newly established, an interconnect adapts to the change by evolving into a stable state, with a single void at the cathode end, and a linear pressure distribution in the rest of the line. This stable state arises from three features of interconnect structures: the aluminide layers shunt the electric current where the void depletes aluminum, the tungsten studs and the oxide prevent aluminum atoms from leaving or entering the line, and the oxide provides the stiffness to contain the pressure. The stable state exists if the electromigration-induced pressure does not break the oxide or cause debond of one of the interfaces. The saturation resistance depends on well controlled variables; attention should be paid to materials and shapes that lower it. Although thermal voids are typically small, the sum of their volumes is significant. Even under a small electric current density, these small voids are gradually filled at the expense of aluminum at the cathode end, leading to a large resistance increase.

Acknowledgements—The work was supported by NSF through grant MSS-9258115. The writer is also grateful to the support of the Institute of Materials Research and Engineering, Singapore, and of the Intel Corp.

REFERENCES

1. Ho, P. S. and Kwok, T., *Rep. Progr. Phys.*, 1989, **52**, 301.
2. Thompson, C. V. and Lloyd, J. R., *MRS Bulletin*, 1993, **19**, .
3. Hu, C-K., Rodbell, K. P., Sullivan, T. D., Lee, K. Y. and Bouldin, D. P., *IBM J. Res. Develop.*, 1995, **39**, 465.

4. Yue, J. T., Funsten, W. P. and Taylor, R. V., in *Proc. Int. Reliability Phys.*, 1985, p. 126.
5. Lytle, S. A. and Oates, A. S., *J. appl. Phys.*, 1992, **71**, 174.
6. Arzt, E., Kraft, O., Nix, W. D. and Sanchez, J. E. Jr, *J. appl. Phys.*, 1994, **76**, 1563.
7. Marieb, T., Flinn, P., Bravman, J. C., Gardner, D. and Madden, M., *J. appl. Phys.*, 1995, **78**, 1026.
8. Hu, C.-K., Small, M. B. and Ho, P. S., *J. appl. Phys.*, 1993, **74**, 969.
9. Filippi, R. G., Biery, G. A. and Wachnik, R. A., *J. appl. Phys.*, 1995, **78**, 3756.
10. Filippi, R. G., Wachnik, R. A., Aochi, H., Lloyd, J. R. and Korhonen, M. A., *Appl. Phys. Lett.*, 1996, **69**, 2350.
11. Jones, R. E. and Basehore, M. L., *Appl. Phys. Lett.*, 1987, **50**, 725.
12. Greenebaum, B., Sauter, A. I., Flinn, P. A. and Nix, W. D., *Appl. Phys. Lett.*, 1991, **58**, 1845.
13. Shen, Y.-L., Suresh, S. and Blech, I. A., *J. appl. Phys.*, 1996, **80**, 1388.
14. Ma, Q., Chiras, S., Clarke, D. R. and Suo, Z., *J. appl. Phys.*, 1995, **78**, 1614.
15. Korhonen, M. A., Borgesen, P., Tu, K. N. and Li, C.-Y., *J. appl. Phys.*, 1993, **73**, 3790.
16. Thouless, M. D., *Scripta mater.*, 1996, **34**, 1825.
17. Blech, I. A., *J. appl. Phys.*, 1976, **47**, 1203.
18. Lange, F. F., *Fracture Mechanics of Ceramics*, Vol. 2. Plenum, New York, 1976, p. 599.
19. Lu, T. C., Yang, J., Suo, Z., Evans, A. G., Hecht, R. and Mehrabian, R., *Acta metall. matter*, 1991, **39**, 1883.
20. Hutchinson, J. W. and Suo, Z., *Adv. appl. Mech.*, 1991, **29**, 64.
21. Ho, S. and Suo, Z., *Acta metall. mater.*, 1992, **40**, 1685.
22. Sanchez, J. E. and Pham, V., *Mat. Res. Soc. Symp. Proc.*, 1994, **338**, 459.
23. Clement, J. J., Lloyd, J. R. and Thompson, C. V., *Mat. Res. Soc. Proc.*, 1995, **391**, 423.